

Facile Synthesis of Magnetophoretic Augmented Adsorbent for Water Remediation

Chuan Chuan Lim ^a, Qi Hwa Ng ^{a,b,*}, Siew Hoong Shuit ^{c,d}, Siti Kartini Enche Ab Rahim ^{a,b}, Peng Yong Hoo ^{a,b}, and Sigit Tri Wicaksono ^e

^aFaculty of Chemical Engineering & Technology, Universiti Malaysia Perlis (UniMAP), Perlis, Malaysia

^bCentre of Excellence for Frontier Materials Research (CFMR), Universiti Malaysia Perlis (UniMAP), Perlis, Malaysia

^cDepartment of Chemical Engineering, Lee Kong Chian Faculty of Engineering & Science, Universiti Tunku Abdul Rahman, Sungai Long Campus, Jalan Sungai Long, Bandar Sungai Long, Cheras, 43000, Kajang, Selangor, Malaysia

^dCentre of Photonics and Advanced Materials Research, Sungai Long Campus, Universiti Tunku Abdul Rahman (UTAR), Jalan Sungai Long, Bandar Sungai Long, Cheras, Kajang 43000, Selangor, Malaysia

^eDepartment of Materials and Metallurgical Engineering, Institut Teknologi Sepuluh Nopember (ITS), Subaraya, Indonesia

*Corresponding author. E-mail: qhng@unimap.edu.my

Received 17 October 2023, Revised 18 December 2023, Accepted 1 January 2024

ABSTRACT

In this new era of globalization, magnetic adsorbents have gained vast attention from researchers in wastewater treatment applications. In this study, sulphonated magnetic multi-walled carbon nanotubes (S-MMWCNTs) were used to remove methylene blue (MB) from an aqueous solution. The S-MMWCNTs are characterized by various analytical methods to investigate their adsorbent features. Adsorption behaviours of the as-prepared composites affected by solution pH and contact time were systematically studied and discussed. The adsorption kinetic data fit the pseudo-second-order kinetic model well. Moreover, the MB removal efficiency of S-MMWCNTs only drops slightly (~6.5%) after five consecutive adsorption cycles, showing their good stability and recyclability.

Keywords: Adsorption, Fe₃O₄, Kinetics, Magnetic adsorbent, Methylene blue, Recyclability

1. INTRODUCTION

Water is an essential natural resource that supports life, food production, economic growth, and well-being [1]. Water pollution has become a severe environmental concern due to rapid population expansion and industrialization [2]. Methylene blue (MB), a synthetic dye, is one of the primary pollutants dumped from the textile industries that cause significant water pollution due to its carcinogenic, toxic, mutagenic, or teratogenic nature, which poses a severe threat to the environment and living organisms [3]. In this sense, the dye-contaminated wastewater must be treated adequately before disposal into the environment.

At present, various separation methods have been developed to remove dye from wastewater, such as coagulation, flocculation, precipitation, ozonation, biological treatment, sedimentation, and adsorption [4], [5]. Adsorption has been verified as the most operative method and has gained significant attention from researchers due to its high removal efficiency, simple operation, low cost, and wide variety of adsorbents [6], [7].

Recently, magnetic adsorbents have become a research hotspot due to their simple and environmentally friendly

separation [8], [9]. Magnetic adsorbents can easily and rapidly separate from the medium by applying a magnetic field, unlike conventional adsorbents, which require additional filtration or centrifugation procedure which is tedious and complicated [10].

The primary purpose of this work is to synthesize sulphonated magnetic multi-walled carbon nanotubes (S-MMWCNTs) by doping the 50-100 nm of iron oxide, Fe₃O₄ nanoparticles with sulphonated multi-walled carbon nanotubes (s-MWCNTs) via the facile solvent-free direct doping method for the removal of MB from an aqueous solution. It is worth noting that in prior research, 30 nm Fe₃O₄ nanoparticles were employed to synthesize S-MMWCNTs [11]. Therefore, this work aims to address a research gap by investigating the impact of Fe₃O₄ nanoparticle size on the formation of magnetic composites and its subsequent effects on adsorption performance. The synthesized S-MMWCNTs were characterized using scanning electron microscopy coupled with energy-dispersive X-ray (SEM-EDX) and X-ray diffraction (XRD). Batch experiments that considered the pH parameter, adsorption time, and kinetic study were conducted. Finally, the regeneration experiment with S-MMWCNTs was undertaken to evaluate the magnetic composite's reusability.

2. MATERIALS AND METHODS

2.1. Materials

The MWCNTs were purchased from Shen Zhen Nanotechnologies Port Co. (China). Magnetite iron oxide Fe₃O₄ (50–100 nm) nanoparticle was supplied by NanoAmor (USA). Concentrated HNO₃ (69%), SYSTERM® was supplied from CLASSIC CHEMICALS (Shah Alam, Selangor, Malaysia). Ammonia sulphate ((NH₄)₂SO₄) was purchased from Qrec (Asia) Sdn. Bhd. (Rawang, Selangor, Malaysia). Methylene blue powder (C.I.52015), StainPur, SYSTERM® were purchased from CLASSIC CHEMICALS (Shah Alam, Selangor, Malaysia).

2.2. Synthesis of S-MMWCNTs

Firstly, surface modification of pristine MWCNTs was carried out by acid-treatment using concentration HNO₃ to form c-MWCNTs and then further functionalized to s-MWCNTs through thermal decomposition of ((NH₄)₂SO₄) as described in previously published work [7], [12]. After that, the synthesized s-MWCNTs were mixed with 50–100 nm-sized Fe₃O₄ nanoparticles to form the S-MMWCNTs composite via facile solvent-free direct doping method, according to the previously published work [11]. 7 mL of 2000 ppm Fe₃O₄ solution was pipetted into the centrifuge bottle with 30 mL of distilled water, and the solution pH was adjusted to 4.5. Next, 21 mg of s-MWCNTs were dispersed into the pH-adjusted Fe₃O₄ solution and sonicated for 5 mins before shaking overnight using an orbital shaker. After shaking overnight, S-MMWCNTs formed were collected by applying a magnetic field to the centrifuge bottle and rinsed with DI water repeatedly. Lastly, S-MMWCNTs were dried in an oven for 12 hours at 100°C.

2.3. Batch Adsorption

A batch adsorption study was carried out by dispersing 20 mg of S-MMWCNTs into 20 mL of a 10 ppm MB solution using a scintillation vial at room temperature. The mixture was then allowed to shake for 1 h at different pHs (pH 3, 7 and 10) for the pH parameter study. The agitation time

range of 1 to 180 min was carried out for the adsorption time study. After adsorption, the S-MMWCNTs suspended in the mixture were isolated from the medium by subjecting the magnetic field to the dispersion. Then, the concentrations of MB remaining after the adsorption process were analyzed using a UV-Vis spectrophotometer. The removal efficiency of MB was then calculated by Equation (1):

$$R = \frac{C_o - C_e}{C_o} \times 100\% \quad (1)$$

where R is the removal efficiency of MB (%), C_o is the initial concentration of MB (mg/L) and C_e is the final concentration of MB (mg/L).

2.4. Characterization of S-MMWCNTs

XRD analysis was performed to investigate the crystalline phase of the bare Fe₃O₄, pristine MWCNTs, s-MWCNTs and S-MMWCNTs using a D2 phaser instrument (Bruker, Germany). Prior to the analysis, the samples were dispersed onto the middle column of a round, transparent glass disc sample holder, and the surface was flattened using a glass plate or ruler to avoid interference with the XRD results. Subsequently, the sample holder was inserted into the XRD chamber and scanned over a range of 2θ angles from 10° to 90° with Cu-K α radiation ($\lambda_{Cu} = 1.5406 \text{ \AA}$) at a tube voltage of 30 kV and a tube current of 10 mA. The surface morphology and chemical composition of bare Fe₃O₄, pristine MWCNTs, s-MWCNTs, and S-MMWCNTs were investigated using SEM-EDX (JEOL, JSM-6460LA, Japan) analysis. Prior to the SEM-EDX analysis test, the samples were coated with a thin layer of gold under vacuum and then analyzed at an operating voltage of 4.0 kV.

3. RESULTS AND DISCUSSION

3.1. Characterization

In this section, S-MMWCNTs were analyzed by XRD and SEM-EDX. The crystalline structure of pristine MWCNTs, bare Fe₃O₄, s-MWCNTs and S-MMWCNTs was investigated using XRD analysis, and their XRD patterns are shown in Figure 1.

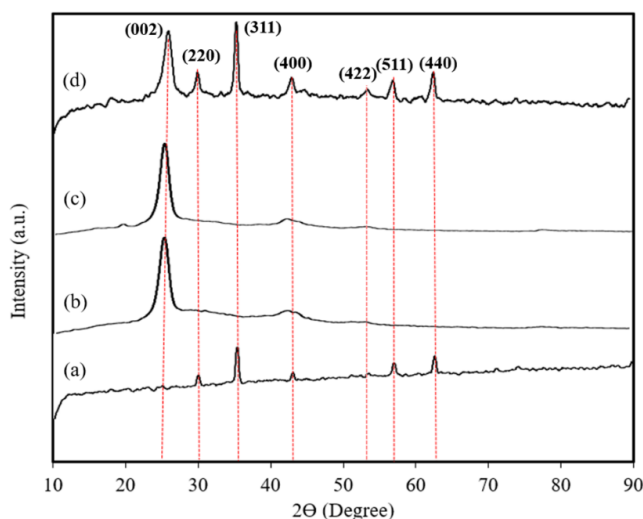


Figure 1. XRD patterns of (a) bare Fe₃O₄, (b) pristine MWCNTs, (c) s-MWCNTs and (d) S-MMWCNTs

The XRD pattern of bare Fe_3O_4 as shown in Figure 1 (a) consisted of six diffraction peaks at 2θ values of 30.39° , 35.53° , 43.32° , 53.61° , 57.23° and 62.79° , corresponding to (220), (311), (400), (422), (511) and (440) diffraction planes, respectively. These observed diffraction peaks matched the phase magnetite JCPDS no. 01-085-1436, indicating that the bare Fe_3O_4 used in this study had a cubic spinel structure [11]. This diffraction pattern of bare Fe_3O_4 with the size of 50-100 nm is in accordance with the bare Fe_3O_4 with the size of 30 nm used in previously published work, even though the particle size is different [11], [13]. On the other hand, a sharp peak at 26.27° (002) was detected for the XRD pattern of pristine MWCNTs, as shown in Figure 1 (b), assigned to the graphitic tubular structure of the carbon atoms [14]. Interestingly, the XRD pattern of s-MWCNTs (Figure 1 (c)) is found to be identical to the XRD pattern of pristine MWCNTs (Figure 1 (b)), which indicates the functionalization process of MWCNTs did not alter or disrupt the original graphitic structure of MWCNTs. Regarding the XRD pattern of S-MMWCNTs (Figure 1 (d)), all the diffraction peaks from bare Fe_3O_4 and pristine MWCNTs were found to coexist, indicating that the bare Fe_3O_4 nanoparticles were successfully doped onto the s-MWCNTs without altering the crystalline structure.

Figure 2 shows the SEM images of bare Fe_3O_4 , pristine MWCNTs, s-MWCNTs and S-MMWCNTs. As shown in Figure 2 (a), the surface morphology of bare Fe_3O_4 appeared in a homogenous bulky agglomerate. Figures 2 (b) and (c) show

the surface morphology of MWCNTs before and after functionalization, respectively, where both SEM images were almost the same. Moreover, the bare Fe_3O_4 nanoparticles were found to appear on the surface of s-MWCNTs (highlighted with the red circle) in the SEM image of S-MMWCNT as shown in Figure 2 (d), which proved that the bare Fe_3O_4 nanoparticles were successfully doped onto the s-MWCNTs by the facile solvent-free direct doping method.

Figure 3 shows the elemental analysis of bare Fe_3O_4 , pristine MWCNTs, s-MWCNTs and S-MMWCNTs by EDX. There are two elements detected in bare Fe_3O_4 according to Figure 3 (a), which are Fe (47.78 wt%) and O (52.52 wt%). Besides that, the EDX analysis of s-MWCNTs (Figure 3 (c)) showed the presence of the S element. The appearance of the S element indicates that the sulphonated group ($-\text{SO}_3\text{H}$) was successfully functionalized onto the surface of MWCNTs through sulphonation. In addition, the existence of Ni element found in the pristine MWCNTs (Figure 3 (b)) disappeared in EDX spectra of s-MWCNTs (Figure 3(c)) due to the acid treatment carried out before the sulphonation process, which can purify and remove impurities existing in the pristine MWCNTs [11]. Furthermore, the EDX result of S-MMWCNTs (Figure 3 (d)) showed the presence of Fe elements and an increase in O element composition, which further proved that the bare Fe_3O_4 had been successfully doped onto the s-MWCNTs to form S-MMWCNTs.

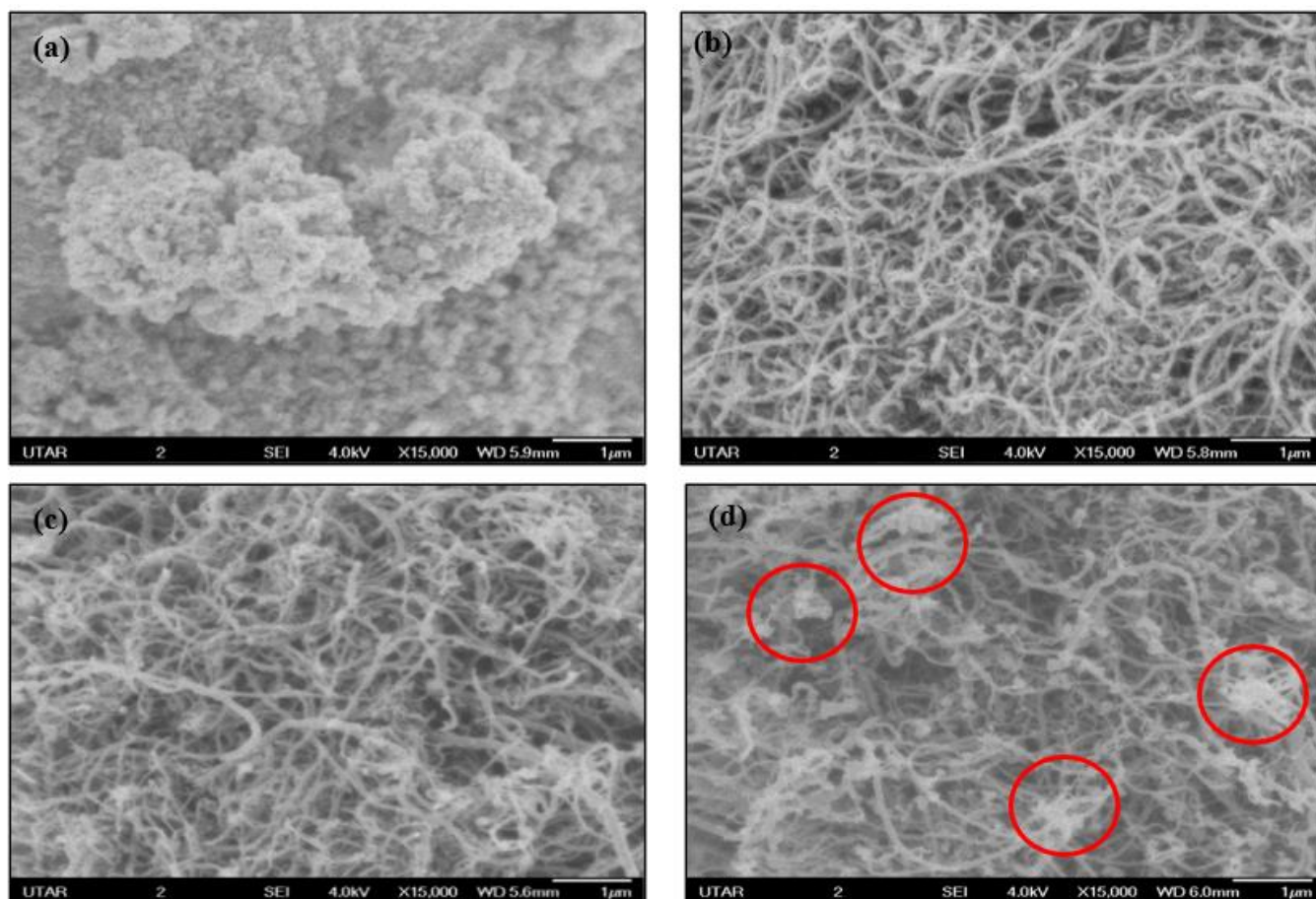


Figure 2. SEM images of (a) bare Fe_3O_4 , (b) pristine MWCNTs, (c) s-MWCNTs and (d) S-MMWCNTs

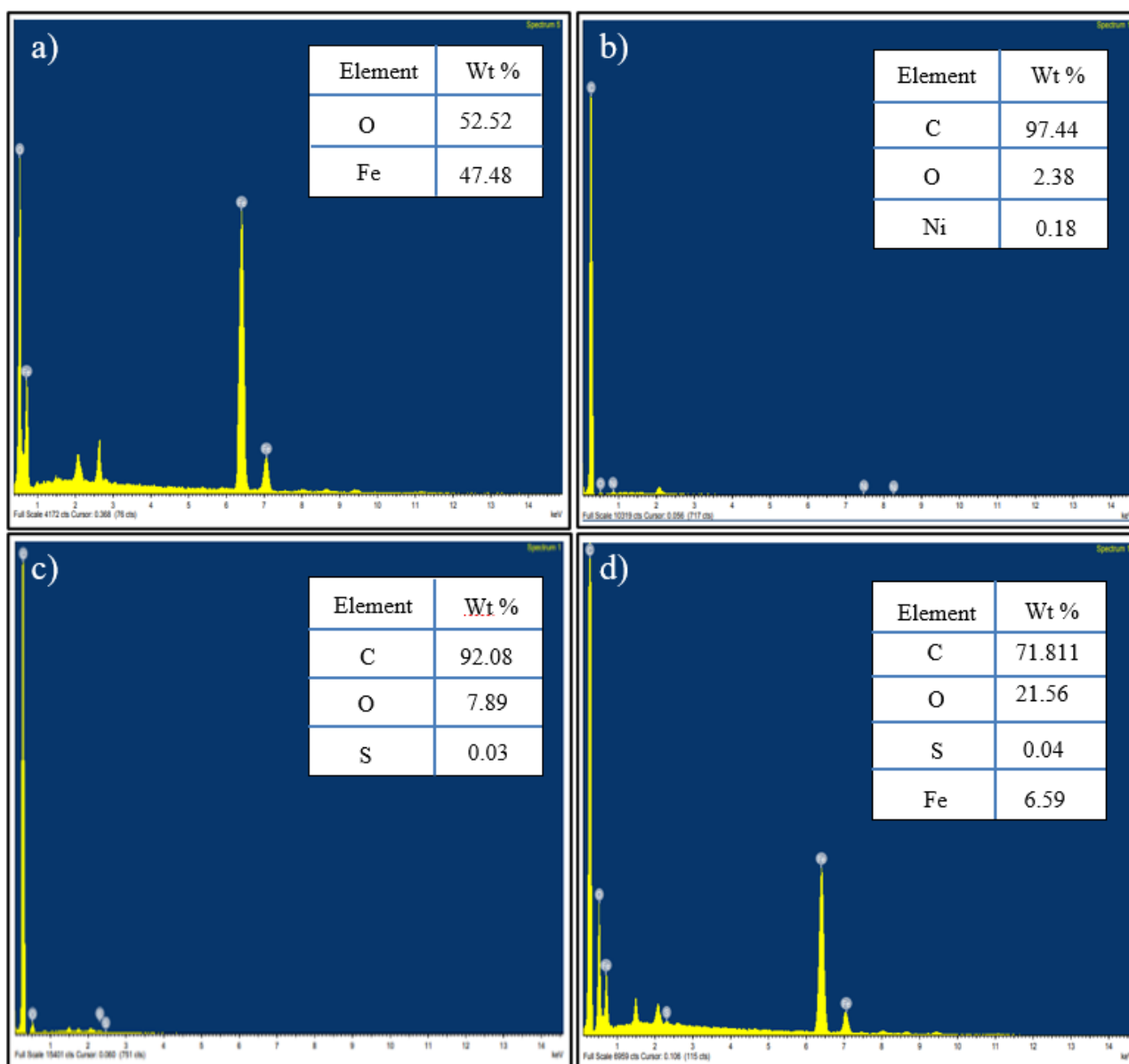


Figure 3. EDX spectrum of (a) bare Fe₃O₄, (b) pristine MWCNTs, (c) s-MWCNTs and (d) S-MMWCNTs

3.2. Adsorption Study of MB

3.2.1. Effect of solution pH

The pH of a solution plays an essential role in affecting the adsorption efficiency by altering the surface charge of the adsorbent. In this sense, the pH solution parameter study was carried out at various pH mediums, which are pH 3 (acidic), pH 7 (neutral) and pH 10 (basic) under constant conditions: 20 mL of 10 ppm MB solution, 20 mg of S-MMWCNTs dosage, 1 h of agitation time and room temperature. Figure 4 shows the MB removal efficiency of S-MMWCNTs at different solution pHs studied. As shown in the figure, the MB removal efficiency increased from pH 3 (77.13%) to pH 10 (93.04%), reflecting that the adsorption of MB by S-MMWCNTs is preferable in basic medium and pH-dependent. Such observation can be explained by the cationic nature of MB, which is favorable to be uptake by the adsorbent at neutral and basic conditions. At pH 3, an acidic medium, cationic MB competes with the hydrogen ions (H⁺) to occupy the active site of the adsorbent [15]. Therefore, at

a pH higher than 7 (neutral or basic medium) lacking or free of H⁺ as the competitor, adsorption of MB onto S-MMWCNTs could achieve higher adsorption efficiency.

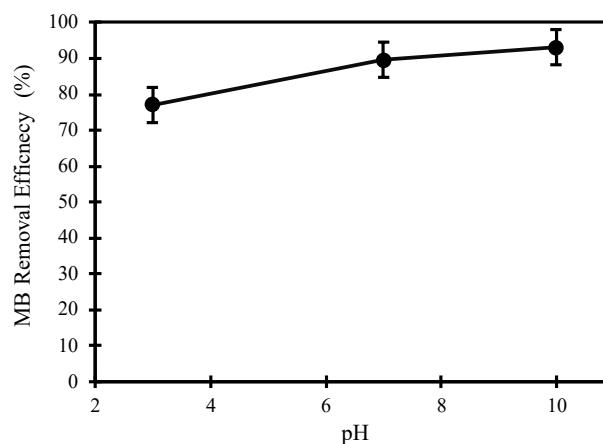


Figure 4. The effect of solution pH on adsorption of MB by S-MMWCNTs

3.2.2. Influence of Adsorption Time on Adsorption and Adsorption Kinetics

The adsorption time study is vital to investigate the time taken for the adsorption to reach equilibrium. In this study, the adsorption time varied from 1, 3, 5, 10, 20, 40, 60, 90, 120, 150, 180 and 210 min, and the adsorption rate versus adsorption time plot is shown in Figure 5. The results show that the MB removal efficiency increased rapidly over the first 60 min and remained almost constant after 150 min.

Furthermore, the MB adsorption kinetics onto S-MMWCNTs were evaluated by the two most common kinetic models, pseudo-first-order and pseudo-second order kinetic models. The equations of pseudo-first-order and pseudo-second-order in linear regression form are expressed in Equations (2) and (3), respectively:

$$\ln(q_e - q_t) = \ln q_e - k_1 t \tag{2}$$

$$\frac{t}{q_t} = \frac{1}{k_2 q_e^2} + \frac{t}{q_e} \tag{3}$$

where q_t and q_e (mg/g) are the amount of MB adsorbed at a given time and equilibrium, respectively; k_1 (min^{-1}) is the rate constant of the pseudo-first-order model, and k_2 ($\text{g}/\text{mg}\cdot\text{min}$) is the rate constant of the pseudo-second-order model. The linear regression plots of these two kinetic models were displayed in Figure 6, whereas the kinetic constants and the correlation coefficient (R^2) were tabulated in Table 1. From the results, the kinetic

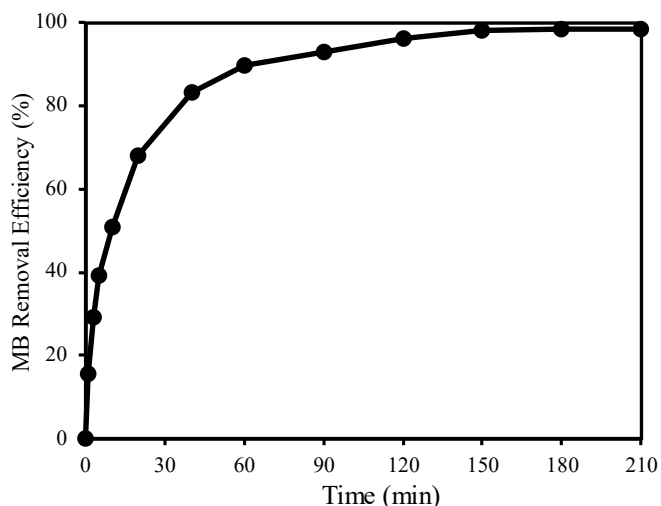


Figure 5. Effect of adsorption time on MB adsorption onto S-MMWCNTs

adsorption data is better fitted to the pseudo-second-order model than the pseudo-first-order model to describe the adsorption behavior of MB adsorption onto S-MMWCNTs due to the higher R^2 value (0.9984) and the closer relation between the calculated q_e (10.152 mg/g) and experimental q_e (9.8380 mg/g) values. Therefore, the adsorption of MB onto S-MMWCNTs obeyed pseudo-second-order, suggesting that the chemisorption interaction caused by electrostatic attraction is the rate-controlling step in the adsorption process [16].

Table 1. Kinetic parameters for the adsorption of MB onto S-MMWCNTs

Experimental	Pseudo-first-order			Pseudo-second-order		
q_e (mg/g)	k_1 (min^{-1})	q_e (mg/g)	R^2	q_e (mg/g)	k_2 ($\text{g}/\text{mg}\cdot\text{min}$)	R^2
9.8380	0.0400	8.5806	0.9559	10.152	0.0150	0.9984

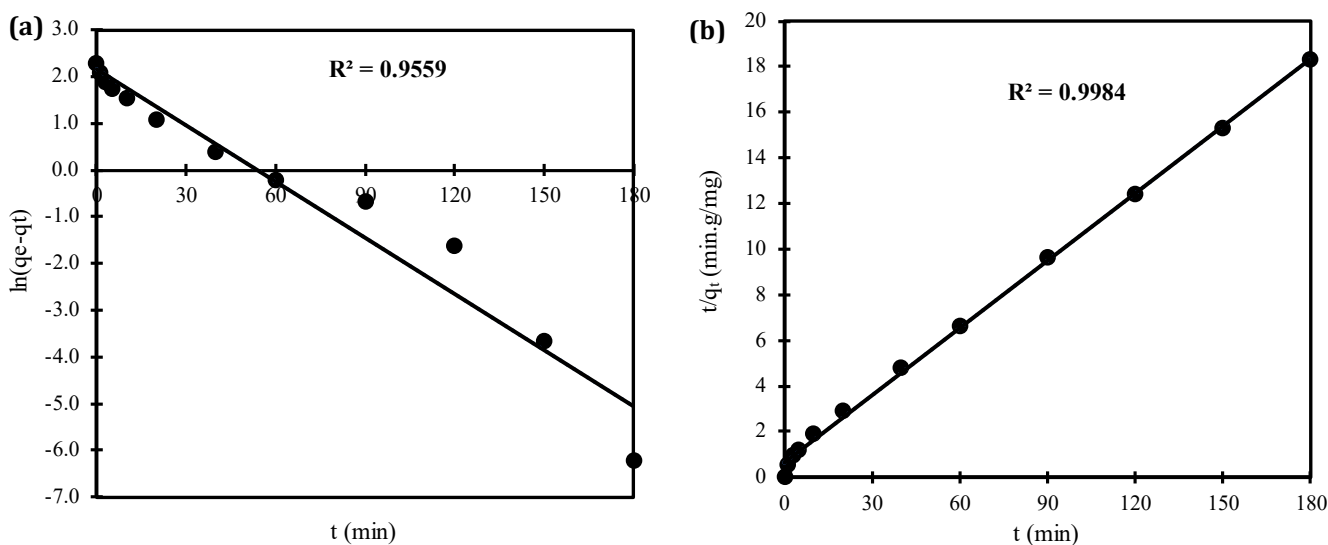


Figure 6. (a) Pseudo-first-order and (b) Pseudo-second-order kinetic plots for the adsorption of MB onto S-MMWCNTs

3.3. Regeneration and Reusability of S-MMWCNTs

As performed in previously published work, the MB adsorbed S-MMWCNTs were regenerated through the Fenton reaction method [11]. Figure 7 displays the reusability results of S-MMWCNTs for five adsorption cycles. The results show that the MB removal efficiency of S-MMWCNTs at the fifth adsorption is still around 80%, with a slight drop (~6.5%) from 86.46%. Therefore, S-MMWCNTs have commercial value for wastewater treatment applications because of their excellent recycling performance.

4. CONCLUSION

In this study, S-MMWCNTs magnetic composite was synthesized successfully using a facile solvent-free direct doping method. XRD and SEM-EDX characterization techniques proved that the bare Fe₃O₄ nanoparticle had been successfully doped onto the surface of s-MWCNTs. The effect of solution pH as an adsorption parameter study showed that the adsorption of MB onto S-MMWCNTs is pH-dependent, and the highest adsorption rate was found at pH 10. In addition, the kinetic studies reveal that the adsorption of MB onto S-MMWCNTs obeys the pseudo-second-order kinetic model. Furthermore, S-MMWCNTs exhibited good stability and recyclable properties as their MB removal efficiency remained at 80%, with a slight drop (~6.5%) after five successive adsorption cycles.

ACKNOWLEDGMENTS

The author would like to acknowledge the support from the Fundamental Research Grant Scheme (FRGS) under a grant number of FRGS/1/2018/TK10/UNIMAP/02/1 from the Ministry of Higher Education Malaysia. Furthermore, sincere indebtedness and gratitude are addressed to the Universiti Malaysia Perlis (UniMAP).

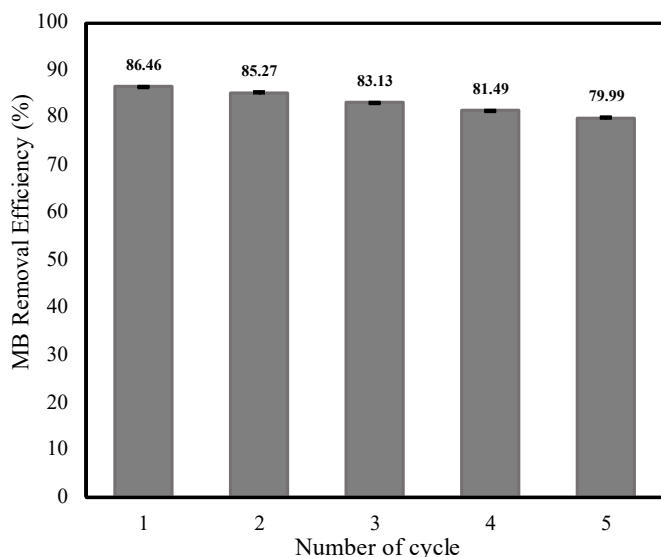


Figure 7. The recovery efficiency of S-MMWCNTs in MB removal for five cycles

REFERENCES

- [1] Z. Kılıç, "The importance of water and conscious use of water," *International Journal of Hydrology*, vol. 4, no. 5, pp. 239–241, Oct. 2020.
- [2] V. Ganesan, C. Louis, and S. P. Damodaran, "Graphene oxide-mesoporous iron oxide nanohybrid: an efficient reusable nano-adsorbent for the removal of organic dyes from wastewater," *Materials Research Express*, vol. 6, no. 8, p. 0850f8, 2019.
- [3] E. Misran, O. Bani, E. M. Situmeang, and A. S. Purba, "Banana stem based activated carbon as a low-cost adsorbent for methylene blue removal: Isotherm, kinetics, and reusability," *Alexandria Engineering Journal*, vol. 61, no. 3, pp. 1946–1955, 2022.
- [4] T. Saeed *et al.*, "Synthesis of chitosan composite of metal-organic framework for the adsorption of dyes; kinetic and thermodynamic approach," *Journal of Hazardous Materials*, vol. 427, p. 127902, 2022.
- [5] J. Wang *et al.*, "Facile synthesis of a magnetic chlorapatite composite with a high efficiency and recyclable adsorption for Congo red," *Materials Research Express*, vol. 6, no. 11, p. 116118, 2019.
- [6] W. H. Chong, Q. H. Ng, J. K. Lim, S. P. Yeap, and S. C. Low, "Study on the enhancement of colloidal stable poly(sodium 4-styrene sulfonate) coated magnetite nanoparticles and regeneration capability for rapid magnetophoretic removal of organic dye," *Journal of Chemical Technology & Biotechnology*, vol. 95, no. 12, pp. 3093–3104, Dec. 2020.
- [7] C. C. Lim, S. H. Shuit, S. K. Enche Ab Rahim, P. Y. Hoo, and Q. H. Ng, "Removal of methylene blue using magnetic multi-walled carbon nanotubes: process optimization study," *IOP Conference Series: Materials Science and Engineering*, vol. 932, no. 1, p. 012015, Sep. 2020.
- [8] Q. H. Ng, J. K. Lim, A. A. Latif, B. S. Ooi, and S. C. Low, "Enhance the Colloidal Stability of Magnetite Nanoparticles Using Poly(sodium 4-styrene sulfonate) Stabilizers," *Applied Mechanics and Materials*, vol. 625, pp. 168–171, Sep. 2014.
- [9] S. Tamjidi, H. Esmaeili, and B. Kamyab Moghadas, "Application of magnetic adsorbents for removal of heavy metals from wastewater: a review study," *Materials Research Express*, vol. 6, no. 10, p. 102004, 2019.
- [10] Z. Shen, Y. Kuang, S. Zhou, J. Zheng, and G. Ouyang, "Preparation of magnetic adsorbent and its adsorption removal of pollutants: An overview," *TrAC Trends in Analytical Chemistry*, vol. 167, p. 117241, 2023.
- [11] C. C. Lim *et al.*, "Sulfonated magnetic multi-walled carbon nanotubes with enhanced bonding stability, high adsorption performance, and reusability for water remediation," *Environmental Science and Pollution Research*, vol. 30, no. 14, pp. 40242–40259, Jan. 2023.
- [12] S. H. Shuit and S. H. Tan, "Feasibility study of various sulphonation methods for transforming carbon nanotubes into catalysts for the esterification of palm fatty acid distillate," *Energy Conversion and Management*, vol. 88, pp. 1283–1289, 2014.

- [13] C. C. Lim *et al.*, "Facial synthesis of colloidal stable magnetic nanoparticles coated with high hydrophilic negative charged poly(4-styrenesulfonic acid co-maleic acid) sodium for water remediation," *Polymers for Advanced Technologies*, vol. 34, no. 4, pp. 1341–1357, 2023.
- [14] F. H. Abdulrazzak, A. F. Alkiam, and F. H. Hussein, "Behavior of X-Ray Analysis of Carbon Nanotubes," H. E.-D. Saleh and S. M. M. El-Sheikh, Eds., Rijeka: IntechOpen, 2019, p. Ch. 7.
- [15] A. A. Nezhad, M. Alimoradi, and M. Ramezani, "One-step Preparation of graphene oxide/polypyrrole magnetic nanocomposite and its application in the removal of methylene blue dye from aqueous solution," *Materials Research Express*, vol. 5, no. 2, p. 25508, 2018.
- [16] N. J. Singh *et al.*, "Alkali-cation-incorporated and functionalized iron oxide nanoparticles for methyl blue removal/decomposition," *Nanotechnology*, vol. 31, no. 42, p. 425703, 2020.